IVYSPRING INTERNATIONAL PUBLISHER

Journal of Cancer

2017; 8(5): 774-785. doi: 10.7150/jca.17550

Research Paper

In Vivo Imaging of Experimental Melanoma Tumors using the Novel Radiotracer ^{68}Ga-NODAGA-Procainamide (PCA)

István Kertész[1*], András Vida[2,3*], Gábor Nagy[4], Miklós Emri[1], Antal Farkas[5], Adrienn Kis[1], János Angyal[6], Noémi Dénes[1], Judit P. Szabó[1], Tünde Kovács[2,3], Péter Bai[2,3,7], György Trencsényi[1,4]✉

1. Department of Medical Imaging, Nuclear Medicine, University of Debrecen, Debrecen, Hungary;
2. Department of Medical Chemisty, University of Debrecen, Debrecen, Hungary;
3. MTA-DE Lendület Laboratory of Cellular Metabolism, Debrecen, Hungary;
4. Scanomed LTD, Debrecen, Hungary;
5. Department of Urology, University of Debrecen, Debrecen, Hungary;
6. Department of Periodontology, University of Debrecen, Debrecen, Hungary;
7. Research Center for Molecular Medicine, University of Debrecen, Hungary.

*Equal contribution.

✉ Corresponding author: György Trencsényi, PhD, University of Debrecen, Department of Medical Imaging, Nuclear Medicine, 4032, Debrecen, Nagyerdei krt. 98. Debrecen, Hungary, E-mail: trencsenyi.gyorgy@med.unideb.hu.

Received: 2016.09.12; Accepted: 2016.11.10; Published: 2017.02.25

Abstract

Purpose: The most aggressive form of skin cancer is the malignant melanoma. Because of its high metastatic potential the early detection of primary melanoma tumors and metastases using non-invasive PET imaging determines the outcome of the disease. Previous studies have already shown that benzamide derivatives, such as procainamide (PCA) specifically bind to melanin pigment. The aim of this study was to synthesize and investigate the melanin specificity of the novel ^{68}Ga-labeled NODAGA-PCA molecule *in vitro* and *in vivo* using PET techniques.

Methods: Procainamide (PCA) was conjugated with NODAGA chelator and was labeled with Ga-68 (^{68}Ga-NODAGA-PCA). The melanin specificity of ^{68}Ga-NODAGA-PCA was tested *in vitro*, *ex vivo* and *in vivo* using melanotic B16-F10 and amelanotic Melur melanoma cell lines. By subcutaneous and intravenous injection of melanoma cells tumor-bearing mice were prepared, on which biodistribution studies and small animal PET/CT scans were performed for ^{68}Ga-NODAGA-PCA and ^{18}FDG tracers.

Results: ^{68}Ga-NODAGA-PCA was produced with high specific activity (14.9±3.9 GBq/μmol) and with excellent radiochemical purity (98%<), at all cases. *In vitro* experiments showed that ^{68}Ga-NODAGA-PCA uptake of B16-F10 cells was significantly ($p \leq 0.01$) higher than Melur cells. *Ex vivo* biodistribution and *in vivo* PET/CT studies using subcutaneous and metastatic tumor models showed significantly ($p \leq 0.01$) higher ^{68}Ga-NODAGA-PCA uptake in B16-F10 primary tumors and lung metastases in comparison with amelanotic Melur tumors. In experiments where ^{18}FDG and ^{68}Ga-NODAGA-PCA uptake of B16-F10 tumors was compared, we found that the tumor-to-muscle (T/M) and tumor-to-lung (T/L) ratios were significantly ($p \leq 0.05$ and $p \leq 0.01$) higher using ^{68}Ga-NODAGA-PCA than the ^{18}FDG accumulation.

Conclusion: Our novel radiotracer ^{68}Ga-NODAGA-PCA showed specific binding to the melanin producing experimental melanoma tumors. Therefore, ^{68}Ga-NODAGA-PCA is a suitable diagnostic radiotracer for the detection of melanoma tumors and metastases *in vivo*.

Key words: B16-F10 tumor; ^{18}FDG; ^{68}Ga-NODAGA-PCA; Melanoma malignum; Positron Emission Tomography, Procainamide.

Introduction

Melanoma malignum is an aggressive form of skin cancers that originates from melanocytes. Its incidence has rapidly increased in the last decades [1]. Despite continuous screening programs for the early detection and excision of the primary tumor, the number of patients and those in advanced stages of the disease increase over time. The aggressiveness of melanomas stems from their ability to rapidly grow towards local capillaries and then to form distant metastases in several organs (*e.g.*: lungs, brain, kidneys, liver, and intestines) even when the primary tumor is small [2]. The presence of melanoma metastases largely reduces the length of survival (the 5-years survival rate is between 5-19%) [3], therefore the early identification and localization of these metastases is crucial for patient survival, wherein medical imaging techniques play pivotal role [4,5].

Among the non-invasive imaging techniques positron emission tomography (PET) is a useful method for the detection and staging of malignances due to its high sensitivity and resolution [6]. The most commonly used radiotracer for imaging primary tumors and metastases is the ^{18}F-Fluoro-2-deoxy-D-glucose (^{18}FDG) [7]. ^{18}FDG is a glucose analogue that accumulates in cells characterized by high metabolic activity such as tumors. Despite the widespread use ^{18}FDG has certain limitations: it is not specific for malignant melanoma, moreover, it is also taken up by inflammatory lesions and the cells of the central nervous system making the distinction between healthy and diseased tissue on PET images difficult [8,9]. These limitations of ^{18}FDG calls for the synthesis and characterization of melanoma-specific tracers that do not accumulate in metabolically active tissues, only in the tumors.

In this study we presented the synthesis and the characterization of a new procainamide-derivative NODAGA-PCA labeled with ^{68}Ga to be used as a melanin-specific PET-tracer. Procainamide (PCA) is the derivative of 4-aminobenzoic acid and it is used for the treatment of cardiac arrhythmias [10,11]. It has been reported that benzamide derivatives (*e.g.*: procainamide) specifically bind to melanin [12-15]. Several studies reported that ^{18}F-labeled benzamide analogues, among others ^{18}F-FPBZA ([^{18}F]N-(2-diethylaminoethyl)-4-[2-(2-(2-fluoroetoxy)ethoxy]benzamide [15], ^{18}F-DAFBA (N-(2-diethylaminoethyl)-4-[^{18}F]fluorobenzamide [16], ^{18}F-5-FPN (^{18}F-5-Fluoro-N-(2-[diethyamino]ethyl)picolamide [17] are promising radiotracers for the *in vivo* imaging of malignant melanoma. However, the preparation of these ^{18}F-labeled radiopharmaceuticals is limited because cyclotron is required for the production of ^{18}F. Generator-based radioisotopes are convenient alternatives to cyclotron produced ^{11}C and ^{18}F [18-20]. The PET-isotope, ^{68}Ga bears close to ideal physical properties (89% β+; $t_{1/2}$ = 67.7 min; E_{av}(β+) = 740 keV), easy, on-site accessibility via commercially available ^{68}Ge/^{68}Ga-generators. Additionally, the conjugation of ^{68}Ga to small, biocompatible molecules is a well-established method and rapidly growing field with numerous applications to modern radiopharmaceutical chemistry [21]. The commonly applied macrocyclic chelators other than DOTA with the ability to efficiently chelate trivalent gallium-ion at room temperature – such as NOTA or NODAGA – can prevent the utilization of elevated temperature which is detrimental in case of thermally unstable precursors.

The aim of this study was to characterize the biological behavior of ^{68}Ga-NODAGA-PCA noninvasively. To attest the melanin specificity of this radiopharmaceutical, *in vitro* and *in vivo* experiments were performed using amelanotic Melur and melanin containing B16-F10 melanoma cells lines. To confirm the tumor specificity of ^{68}Ga-NODAGA-PCA *in vivo*, subcutaneous and pulmonary metastatic animal models were investigated using small animal imaging techniques (miniPET/CT).

Materials and Methods

Chemicals

All commercially available chemicals were of analytical grade and used without further purification. For the radiolabeling studies, TraceSelect Ultra water - Sigma-Aldrich Kft. (Budapest, Hungary) – Ultrapur HCl and Suprapur NaOH*H_2O were obtained from Merck Kft. (Budapest, Hungary). Procainamide hydrochloride and all other chemicals were the product of Sigma-Aldrich Kft. (Budapest, Hungary), if not specifically stated otherwise. NODAGA-NHS ester was purchased from Chematech (Dijon, France).

Conjugation reaction of 4-Amino-N-(2-diethylaminoethyl) benzamide hydrochloride with NODAGA-NHS ester

27.2 mg (100 μmol) from the 4-Amino-N-(2-diethylaminoethyl)benzamide hydrochloride was dissolved in 2 mL of acetonitrile (MeCN) / 0.1 M sodium carbonate buffer (pH 9.5) 3:1. 69.5 mg (95 μmol) of NODAGA-NHS ester was introduced into the mixture. The pH was adjusted between 8.5 and 9 by means of 2% of NaOH and the mixture was stirred for 2 h at room temperature. The resulting NODAGA-conjugated benzamide-analogue (NODAGA-PCA)

was purified by means of semi-preparative RP-HPLC and the collected fractions were lyophilized. The pure product was characterized by analytical RP-HPLC (as described below), ESI-MS (Shimadzu LCMS IT-TOF Mass Spectrometer, Shimadzu Corp., Tokyo, Japan) and ^{1}H-NMR (Bruker WP 360 SY).

Radiolabeling of NODAGA-PCA with Ga-68

We have performed the optimization of the radiosynthesis both at room- and at elevated temperature. Due to our compound proved to be not heat-sensitive and the higher temperature granted higher specific activity, therefore for the animal experiments we have produced the radiotracer exclusively at 95°C. This labeling protocol is based on the procedure described by Wängler et al. [22]. ^{68}Ge/^{68}Ga-generator (Obninsk, Eckert & Ziegler, Germany) was eluted with 0.1 M HCl (aq). A fraction of 1 mL volume containing the highest activity (≈ 350 MBq) was collected, buffered with sodium-acetate (1M; 0.15 mL, aq.) and the pH of the stock solution was adjusted to ~ 4.5 by the addition of NaOH (2 %, 0.06 mL, aq.). Then, 5 µL of a 3 mM NODAGA-PCA stock-solution was added and the mixture was incubated for 5 min at 95°C. Afterwards, the reaction mixture was transferred onto a preactivated Oasis HLB 1 cc cartridge (30 mg sorbent). After immobilization of the radioactivity from the mixture, the column was washed with 2 mL of water and then retained activity was recovered with 0.5 mL isotonic NaCl solution/EtOH 2:1. The radiotracer-solution was further diluted with 2 mL isotonic NaCl solution to decrease the alcohol content below 10 % and it was sterile filtered. The specific activity of the product varies between 13-18 GBq/µmol. The radiochemical purity (%) of the final product was determined by application of an analytical RP-HPLC.

Preparative and analytical RP-HPLC methods

The purification of the NODAGA-PCA was performed on a KNAUER HPLC system using a semi-preparative Supelco Discovery® Bio Wide Pore C18 column (150 mm x 10 mm; 10 µm diameters), with a flow rate of 4.4 mL/min. After a short isocratic period (3 min) a linear gradient was used (3 min 0 % B; 20 min 50 % B) with eluent A (0.1% TFA in water) and eluent B (0.1% TFA in MeCN-H_2O (95:5, v/v), applying 254 nm for peak detection.

For the quality control of the radiolabeled compound a similar configuration of KNAUER HPLC - extended with a radiodetector - was used. For analytical purposes a Supelco Discovery® Bio Wide Pore C18 column (250 mm x 4.6 mm) 10 µm diameters was equipped and 1 mL/min flow rate was applied, with a gradient profile: 0 min 0% B, 3 min 0 % B; 20 min 50 % B. Signals were simultaneously detected by radiodetector and UV detector (254 nm).

Determination of partition coefficient of ^{68}Ga-NODAGA-PCA

The partition coefficient of ^{68}Ga-NODAGA-PCA was expressed as log*P* by measuring the distribution of radioactivity in 1-octanol and PBS-solution (pH =7.4). Approximately 1.5 MBq of ^{68}Ga-NODAGA-PCA in 10 µL aq. solution was added to an Eppendorf-vial containing 0.5 mL of PBS and 0.5 mL of 1-octanol. After vigorously vortexing of the mixture for 20 min, the vial was centrifuged at 20.000 rpm for 5 min in order to reach complete separation of layers. 100 µL of each layer was transferred into test tubes; the radioactivity was measured with a gamma counter (Perkin-Elmer Packard Cobra, Waltham, MA, USA). Log*P* value was determined from the results of six experiments.

Determination of *in vitro* stability of ^{68}Ga-NODAGA-PCA

The stability of ^{68}Ga-NODAGA-PCA was tested in mouse serum at 37°C. Approximately 8 MBq of ^{68}Ga-NODAGA-PCA was introduced into mouse serum and was incubated. For serum stability study, 50 µL aliquot of ^{68}Ga-NODAGA-PCA at various time points (0, 30, 60, 90 and 120 min) was mixed with 50 µL cold abs. EtOH. Precipitate was pelleted by centrifugation at 20.000 rpm for 5 min. The supernatant was collected, further diluted with water and the radiochemical purity of ^{68}Ga-NODAGA-PCA was determined by means of the analytical RP-HPLC.

Cell culture

B16-F10 (mouse melanotic melanoma) and Melur (human amelanotic melanoma) cell lines were purchased from the American Type Culture Collection (ATCC). Cells were grown in Dulbecco's Modified Eagle Medium (DMEM High Glucose - GlutaMAX™ - Pyruvate) supplemented with 10% fetal bovine serum (FBS), 1% non-essential amino acid solution (Sigma Aldrich, cat.: M7145) and 1% MEM vitamin solution (Sigma Aldrich) at regular conditions (5% CO_2, 37 °C).

For the *in vitro* studies and animal experiments the cells were used after 6-8 passages and 80% confluence at T75 culture flasks. The viability of the cells used in our experiments was always higher than 90%, as assessed by the trypan blue exclusion test.

In vitro ^{68}Ga-NODAGA-PCA uptake and efflux studies

B16-F10 and Melur cells were trypsinized, centrifuged and resuspended in PBS containing 1 mM glucose (gl-PBS). The samples were preincubated at

37 °C for 10 min at a cell concentration of 1×10^6 ml^{-1} in gl-PBS. 0.37 MBq/ml ^{68}Ga-NODAGA-PCA was then added to each sample. After the addition of the radiotracer, cells were further incubated at 37 °C for 30 and 90 min. After the incubation time, samples were washed 3 times with ice-cold PBS and resuspended in 1 ml of ice cold PBS. Afterwards, radioactivity was measured with Canberra Packard gamma-counter for 1 min within the ^{68}Ga-sensitive energy window.

For the investigation of ^{68}Ga-NODAGA-PCA efflux the samples were first loaded with ^{68}Ga-NODAGA-PCA (at 37 °C for 30 and 90 min) and then washed with gl-PBS at room temperature. Subsequent centrifugation the supernatant was removed and the cells were resuspended in 2 ml 37°C gl-PBS and further incubated for 10 min at 37 °C. The efflux was terminated by the addition of ice-cold PBS. The cells were then washed twice with ice cold PBS and the radioactivity was measured in the gamma-counter for 1 min within the ^{68}Ga-sensitive energy window. Decay-corrected radiotracer uptake was expressed as counts min^{-1} (10^6 cells)$^{-1}$ (cpm). The displayed data represents the means of at least three independent experiments (± SD) carried out using different cell passages, and each experiment was performed in triplicate.

In vivo tumor models

For the establishment of melanoma tumor models adult female C57BL/6 (n=25) and CB17 SCID (n=20) (from Charles River Laboratories by Innovo Kft., Hungary) were used at 8-10 weeks of age. To generate lung-metastasis and subcutaneous tumors, C57BL/6 mice were injected with 1x10^5 B16-F10 tumor cells in 0.9% NaCl (100 µl) intravenously or subcutan into the left shoulder area. For the induction of amelanotic tumor model CB17 SCID mice were used; 1x10^5 amelanotic Melur tumor cells in 100 µl *saline* were injected into the left shoulder area of SCID mice. The growth of subcutaneous tumors was assessed by caliper measurements and tumor size was calculated using the following formula: (largest diameter x smallest diameter^2)/2. *In vivo* experiments were carried out approximately 20 days after intravenous and subcutaneous injection of tumor cells at the tumor volume of 100-120 mm^3.

Animal PET/CT imaging

Control and tumor-bearing animals were injected with 7.0±0.2 MBq of ^{68}Ga-NODAGA-PCA or ^{18}FDG *via* the tail vein 20±2 days after the implantation of B16-F10 or Melur cells. 90 min after ^{68}Ga-NODAGA-PCA and 60 min after ^{18}FDG injection mice were anaesthetized by 3% isoflurane (Forane) with a dedicated small animal anesthesia device and whole body PET scans (10 min acquisition time) were acquired using the MiniPET-II scanner [23]. Scanner normalization and random correction were applied on the data and the images were reconstructed with the standard EM iterative algorithm. The voxel size was 0.5x0.5x0.5 mm and the spatial resolution varies between 1.4 to 2.1 mm from central to 25 mm radial distances. For the anatomical localization of organs and tumors cone-beam computer tomography (CBCT, 3D Accuitomo, Japan) scans were used as we described earlier [24]. Briefly, the X-ray tube settings were voltage 60 kVp, current 8.0 µA, and exposure time 30.8 s per projection; voxel size: 160 µm.

Quantitative PET data analysis

Quantitative radiotracer uptake was expressed in terms of standardized uptake value (SUV), SUV = [VOI activity (Bq/mL)]/[injected activity (Bq)/animal weight (g)], assuming a density of 1 g/mL. Volumes of interest (VOI) were manually drawn around the edge of the organ or tumor activity by BrainCad software [24]. Tumor-to-muscle (T/M) and tumor-to-lung (T/L) ratios were computed as the ratio between the activity in the tumor VOI and in the background (muscle or lung) VOI. Healthy lung from control mouse was used for the calculation of T/L ratio.

Ex vivo biodistribution studies

One day after *in vivo* imaging studies, animals were injected intravenously with 7.0±0.2 MBq of ^{68}Ga-NODAGA-PCA or ^{18}FDG. Mice were euthanized with 5% isoflurane 90 and 60 min after the injection of ^{68}Ga-NODAGA-PCA and ^{18}FDG, respectively. As we described earlier, tissue samples were taken from each organ and their weight and radioactivities were measured with gamma counter and DAR (Differential Absorption Ratio) values were calculated [24].

Data analysis

Significance was calculated by Mann-Whitney U-test and the significance level was set at $p \leq 0.05$ unless otherwise indicated. Data are presented as mean±SD of at least three independent experiments.

Results

Chemical and radiochemical synthesis

The NODAGA-PCA was prepared by a conjugation reacting between 4-Amino-N-(2-diethylaminoethyl)benzamide hydrochloride and NODAGA-NHS ester (Fig 1.). The purity of NODAGA-PCA was more than 99% after semi-preparative RP-HPLC. ^{1}H-NMR (DMSO d-6)δ = 1.27-1.32 (t, 6H), 2.05-2.25 (m, 2H), 2.65-2.68 (t, 2H),

3.07-3.1 (m, 4H), 3.15-3.25 (m, 8H), 3,28-3,32 (m, 4H), 3.35-3.42 (m, 2H), 3.6-3.65 (t, 1H), 3.7-3.85 (m, 6H), 7.55-7.65 (d, 2H), 7.75-7.85 (d, 2H). The purified product was identified by ESI-MS also and found it $[M + H]^+$=593.32 as calculated. The analysis of the MS spectrum verified the expected structure. The overall synthesis time of ^{68}Ga-NODAGA-PCA was 15 min. including the reformulation. The average decay-corrected yield was 68.1±6.7% (n=7) and the radiochemical purity exceeded 98% in every case. The specific activity of the radiotracer was 14.95±3.9 GBq/μmol.

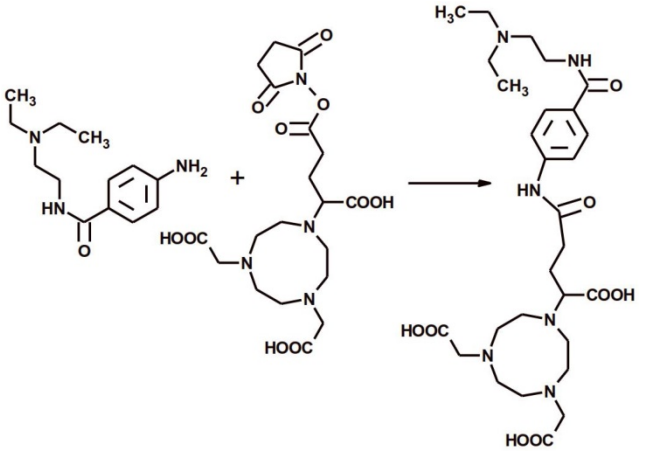

Figure 1. The reaction scheme of the chemical synthesis of NODAGA-PCA.

Partition coefficient and *in vitro* stability of ^{68}Ga-NODAGA-PCA

The partition coefficient (log*P*) of ^{68}Ga-NODAGA-PCA was determined to be -2.79±0.10, suggesting that the radiotracer is highly hydrophilic. Moreover, the stability of the labeled molecule was measured in mouse serum at 37°C using analytical radio-HPLC. After 2 hours of incubation in mouse serum, more than 95 % of the original labeled compound remained intact. These latter results suggest a highly stable molecule under the applied conditions.

In vitro uptake and efflux studies

The melanin specificity of ^{68}Ga-NODAGA-PCA was investigated under *in vitro* conditions using melanin positive B16-F10 and melanin negative Melur cell lines. After 30 and 90 min incubation time significant (p≤0.01) differences were observed between the melanin positive (1.66±0.43 at 30 min; 2.60±0.72 at 90 min) and negative (0.12±0.04 at 30 min; 0.14±0.06 at 90 min) cell lines (Fig. 2). In the efflux studies significant (p≤0.01) differences were also found between the tracer accumulation of melanin positive and negative cell lines. In these washout experiments, cells were first loaded with ^{68}Ga-NODAGA-PCA, followed by extensive washing rounds, and then cells were further incubated for 10 min without radioactivity. The melanin-containing B16-F10 cell line showed significantly higher ^{68}Ga-NODAGA-PCA content at both time points (0.78±0.15 at 30 min; 1.42±0.43 at 90 min) than the melanin-negative Melur cell line (0.08±0.04 at 30 min; 0.08±0.02 at 90 min) (Fig. 2). The radiotracer content in B16-F10 cell line was approximately 13-fold higher at 30 min and 18-fold higher at 90 min than in Melur cells. These differences did not change considerably with the efflux, after 30 and 90 min incubation time followed by 10 min efflux, the radiotracer uptake of B16-F10 cells were 9-fold higher at 30 min and 17-fold higher at 90 min than amelanotic Melur cells.

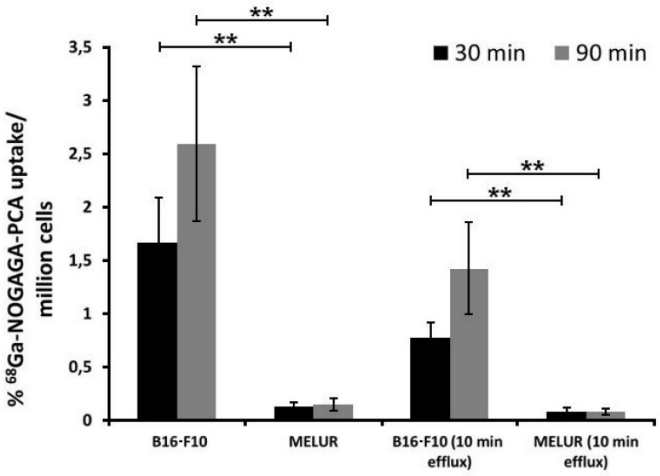

Figure. 2. Comparison of time dependent *in vitro* ^{68}Ga-NODAGA-PCA uptake and efflux (washout kinetic) of melanotic (B16-F10) and amelanotic (Melur) melanoma cell lines. Significance level: p≤0.01 (**). The displayed data are the means ± SD of the results of at least three independent experiments, each performed in triplicate.

In vivo and *ex vivo* biodistribution studies in healthy animals

In vivo imaging and *ex vivo* biodistribution studies were performed using healthy C57BL/6 mouse as controls. 90 min after the injection of 7.0±0.2 MBq of ^{68}Ga-NODAGA-PCA the biodistribution was evaluated by whole body miniPET scans. Representative decay-corrected coronal miniPET/CT image is shown in Fig. 3A. In control animals low accumulation was observed in the abdominal organs and tissues (liver, spleen, intestines) and in the thoracic region. The urinary system (kidneys and urine) were clearly visualized 90 min after tracer injection (Fig. 3A).

These *in vivo* miniPET/CT biodistribution results correlated well with the *ex vivo* data summarized in Fig. 3B. For the *ex vivo* organ and tissue distribution

studies the animals were sacrificed 90 min after the ^{68}Ga-NODAGA-PCA injection, dissected, and the accumulated activities of the tissues and organs were counted with gamma counter. 90 min after the injection of ^{68}Ga-NODAGA-PCA the DAR values of kidneys (0.51±0.19) and urine (53±8.24) showed high tracer accumulation in control mice. In contrast, very low tracer uptake was measured in the liver (0.07±0.02), intestines (0.04±0.01), spleen (0.03±0.01), stomach (0.03±0.01), lung (0.02±0.01) and muscle (0.01±0.005).

In vivo and *ex vivo* biodistribution studies on subcutaneous tumor models

The melanin specificity of ^{68}Ga-NODAGA-PCA was investigated by *in vivo* and *ex vivo* studies using subcutaneously growing melanotic B16-F10 and amelanotic Melur tumors 20±2 days after tumor cell inoculation.

Decay-corrected representative axial images of experimental melanoma tumors are shown on Fig. 4. B16-F10 tumors were clearly visualized with the melanin specific ^{68}Ga-NODAGA-PCA 90 min after the tracer injection (Fig. 4B and C). After the quantitative analysis of PET images significant differences (at $p \leq 0.01$ level) were found in the SUV values of the investigated B16-F10 and Melur tumors. The SUVmean, SUVmax, T/M SUVmean and T/M SUVmax values of the melanin producing B16-F10 tumors were 0.35±0.09, 2.03±0.87, 11.3±2.28 and 13.99±3.25, respectively. Additionally, these values were significantly higher ($p \leq 0.01$) than the tracer uptake of amelanotic Melur tumors, where the SUVmean, SUVmax, T/M SUVmean and T/M SUVmax values were 0.07±0.03, 0.30±0.06, 1.12±0.25 and 0.97±0.14, respectively, confirming the melanin binding specificity *in vivo* (Fig. 4G).

To investigate the melanin specificity of ^{68}Ga-NODAGA-PCA in subcutaneously growing B16-F10 and amelanotic Melur tumors, we performed *ex vivo* biodistribution studies at 90 min post injection. Table 1 demonstrates that the ^{68}Ga-NODAGA-PCA uptake of B16-F10 tumor was significantly ($p \leq 0.01$(**)) higher than that of Melur tumor. This approximately thirty-fold higher accumulation in B16-F10 melanoma confirmed the melanin binding specificity of the radiotracer *ex vivo*. By taking the tumor-to-muscle (background) ratios, the difference between the two tumors was also significant at $p \leq 0.01$ (Table 1).

Table 1. ^{68}Ga-NODAGA-PCA uptake (DAR) in s.c. B16-F10 and Melur tumors 90 min after tracer injection and 20±2 days after tumor cell inoculation. Significance level between B16-F10 and Melur data: $p \leq 0.01$ (**).

Organ/tissue	B16-F10 (n=5)	Melur (n=5)
Tumor (*s.c.*)	0.31 ± 0.04**	0.01 ± 0.01
Tumor/muscle	16.86 ± 3.14**	1.29 ± 0.31

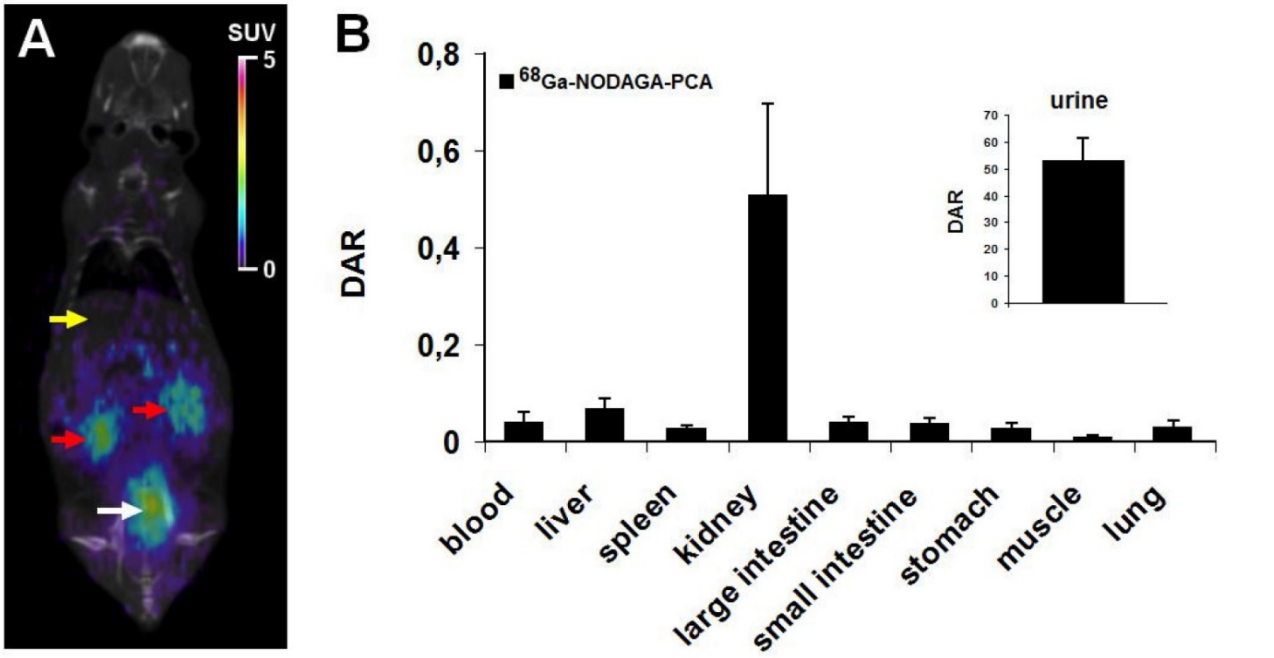

Figure 3. *In vivo* and *ex vivo* biodistribution data for ^{68}Ga-NODAGA-PCA. A: Representative coronal miniPET/CT image of healthy control C57BL/6 mouse 90 min after the radiotracer injection. Yellow arrow: liver; red arrows: kidneys; white arrow: bladder with urine. B: quantitative analysis of tracer uptake in control animals (n=5) 90 min after the injection of ^{68}Ga-NODAGA-PCA. DAR values are presented as mean±SD.

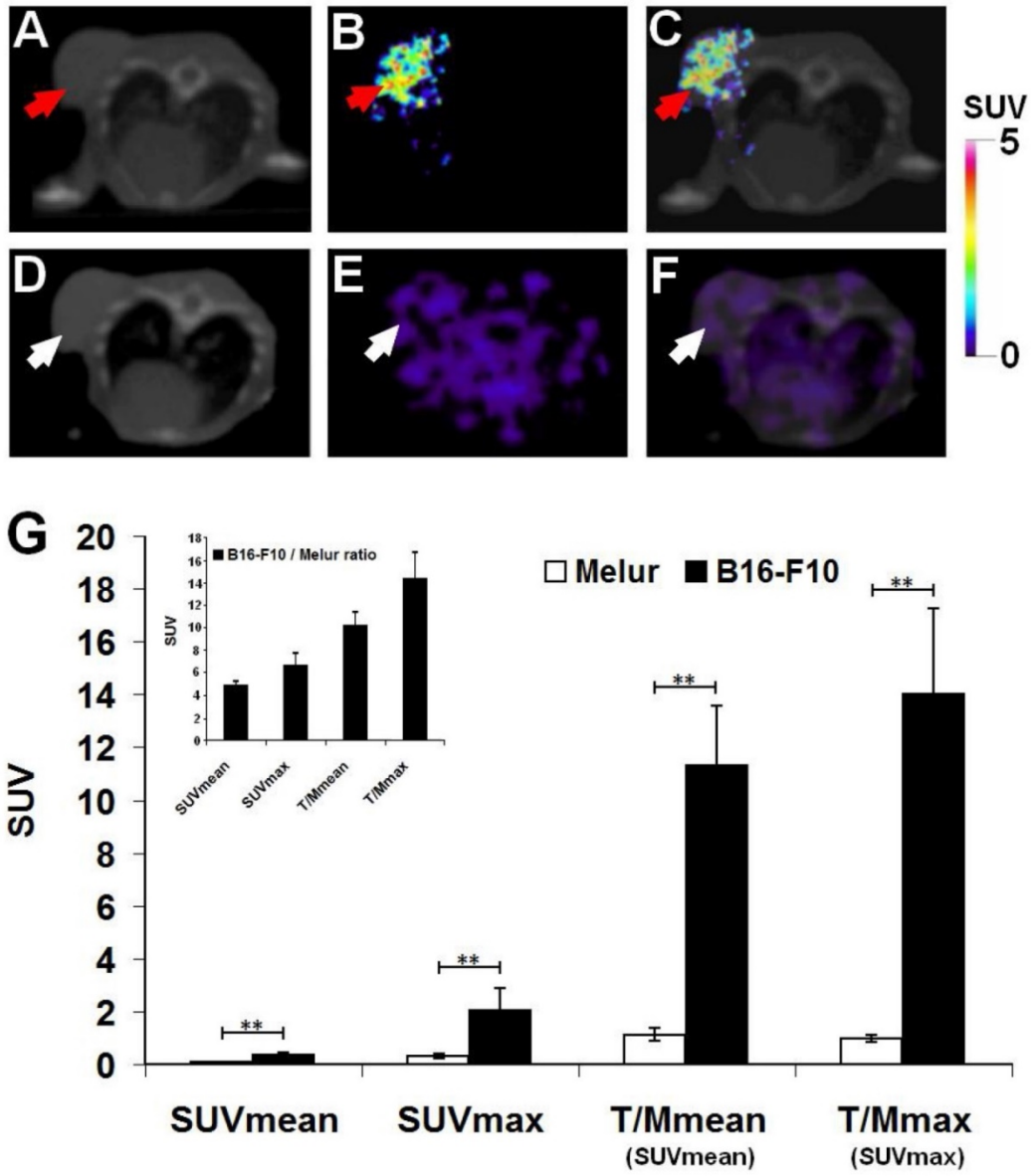

Figure 4. Comparison of *in vivo* accumulation of ^{68}Ga-NODAGA-PCA in B16-F10 (A-C) and Melur (D-F) tumors 90 min after the tracer injection. Representative axial CT (A, D), miniPET (B, E) and miniPET/CT (C, F) images of the subcutaneously growing melanin positive B16-F10 (red arrows) and amelanotic Melur (white arrows) tumors. G: quantitative analysis of the *in vivo* tracer uptake in B16-F10 (n=5) and Melur (n=5) tumors. Insert: ^{68}Ga-NODAGA-PCA uptake ratios of B16-F10 and Melur tumors. Data are presented as mean ± SD. T/M: Tumor/Muscle ratio. Significance level: $p \leq 0.01$ (**).

The accumulation of ^{68}Ga-NODAGA-PCA and ^{18}FDG in melanoma tumors growing under the skin was compared by miniPET scans 90 and 60 min after radiotracer injection, respectively (Fig. 5). Subcutaneously growing B16-F10 and Melur tumors were clearly visualized with the most commonly used non-specific ^{18}FDG. By using the melanin specific radiotracer ^{68}Ga-NODAGA-PCA, we found high accumulation in melanin containing B16-F10 tumors, and a good contrasted image with low background activity was obtained. In contrast, the melanin negative Melur tumors showed very low ^{68}Ga-NODAGA-PCA accumulation (Fig. 5A).

After the quantitative analysis of PET images, B16-F10 melanoma tumors showed significantly ($p \leq 0.01$) higher ^{18}FDG uptake (SUVmean: 4.79±0.88, SUVmax: 10.35±2.7) than ^{68}Ga-NODAGA-PCA accumulation (SUVmean: 0.35±0.09, SUVmax: 2.03±0.87). In contrast, when the ^{68}Ga-NODAGA-PCA uptake data of the tumors were compared to the background (muscle) activity, we found that the T/M SUVmean and T/M SUVmax were 11.3±2.28 and 13.99±3.25, respectively. These values were approximately two- or three-fold higher than that of the ^{18}FDG uptake ratios, where the T/M SUVmean and T/M SUVmax values were 5.27±0.81 and 4.83±1.17, respectively (Fig. 5B). By analyzing the PET images of Melur tumors, significantly ($p \leq 0.01$) higher

^{18}FDG uptake (SUVmean: 0.92±0.10, SUVmax: 1.51±0.11, T/M SUVmean: 4.42±0.58 and T/M SUVmax: 3.27±0.23) was observed than using the melanin specific ^{68}Ga-NODAGA-PCA (Fig. 5C).

In vivo and *ex vivo* biodistribution studies on B16-F10 lung-metastatic tumor model

The accumulation of ^{18}FDG and ^{68}Ga-NODAGA-PCA was compared in B16-F10 lung metastases by small animal PET scans 20±2 days after intravenous injection of tumor cells. Representative decay-corrected axial miniPET/CT images of control and tumor-bearing mice are shown in Fig. 6. The metastatic lesions in the lungs were clearly visualized with both radiotracers (Fig. 6B and C). After the quantitative analysis of PET images it was found that the SUV values of FDG uptake (SUVmean: 2.14±0.7 and SUVmax: 5.26±1.27) were significantly (p≤0.01) higher than that of the melanin specific ^{68}Ga-NODAGA-PCA uptake (SUVmean: 0.15±0.04, SUVmax: 0.42±0.06) (Fig. 6H). However, by analyzing the tumor-to-muscle (T/M) and tumor-to-lung (T/L) ratios the ^{68}Ga-NODAGA-PCA uptake ratios were significantly (p≤0.05 and p≤0.01) higher than the ^{18}FDG accumulation ratios. ^{68}Ga-NODAGA-PCA uptake in B16-F10 lung metastases were approximately six- and eight-fold higher than that of the lung (T/L SUVmean: 6.66±0.43, T/L SUVmax: 8.4±0.77) or muscle (T/M SUVmean: 7.66±0.78, T/M SUVmax: 8.2±0.94) uptake. By using ^{18}FDG, these ratios were lower (T/M SUVmean: 3.32±0.62; T/M SUVmax: 4.3±0.68; T/L SUVmean: 2.15±0.21; T/L SUVmax: 3.68±0.48) than that of the uptake ratios of ^{68}Ga-NODAGA-PCA (Fig. 6H).

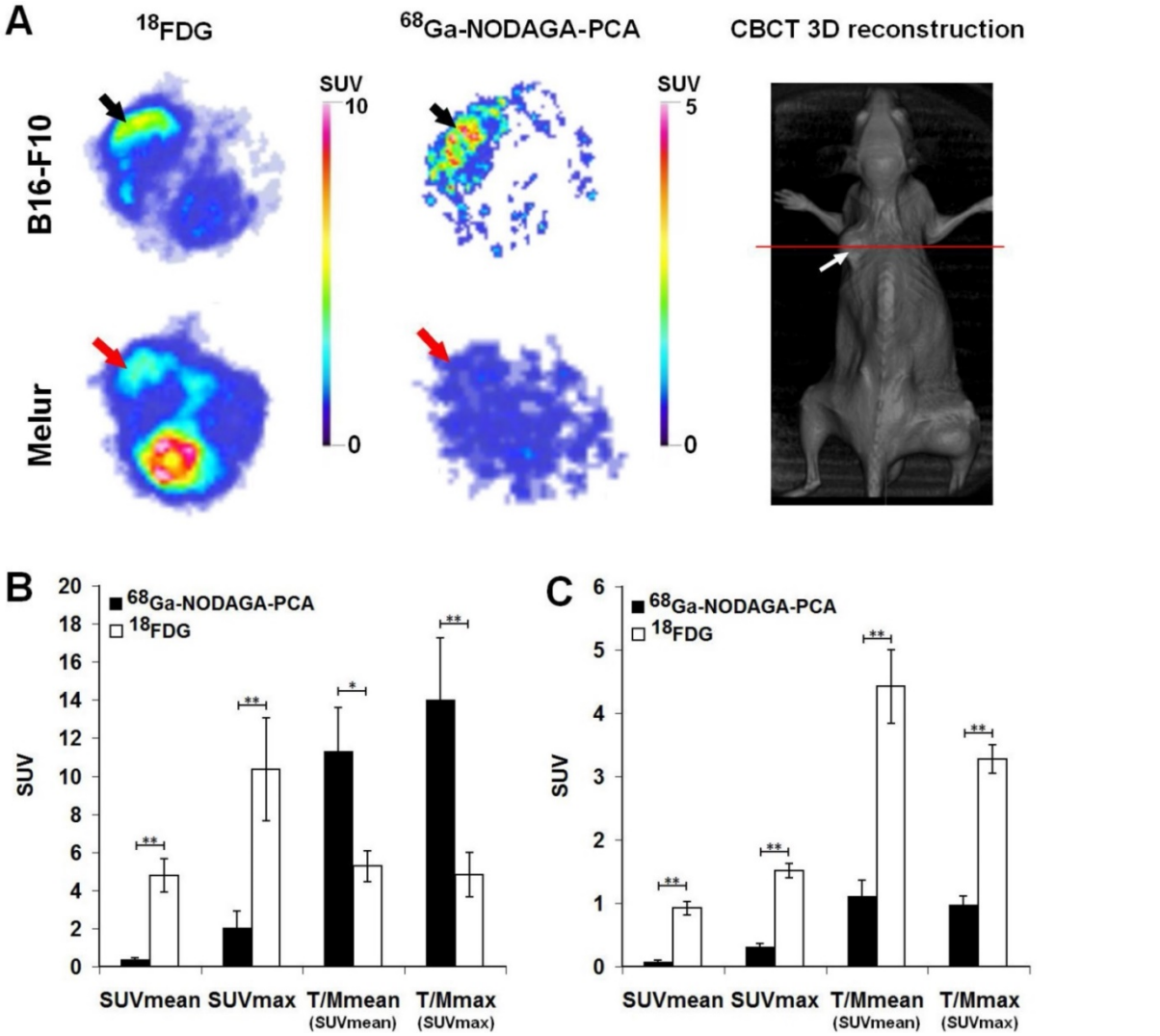

Figure 5. A: Representative axial miniPET images of the same B16-F10 (black arrows) and Melur (red arrows) tumors after the injection of ^{68}Ga-NODAGA-PCA and ^{18}FDG 20 and 21 days after subcutaneous injection of tumor cells. Red line on CBCT image shows the position of the selected axial slices for PET. White arrow: subcutaneously growing Melur tumor. B: quantitative analysis of *in vivo* radiotracer accumulation in B16-F10 (n=5) tumors 90 and 60 min after ^{68}Ga-NODAGA-PCA and ^{18}FDG injection, respectively. C: quantitative analysis of *in vivo* radiotracer accumulation in amelanotic Melur (n=5) tumors 90 and 60 min after ^{68}Ga-NODAGA-PCA and ^{18}FDG injection, respectively. Significance level: p≤0.05 (*); p≤0.01 (**).

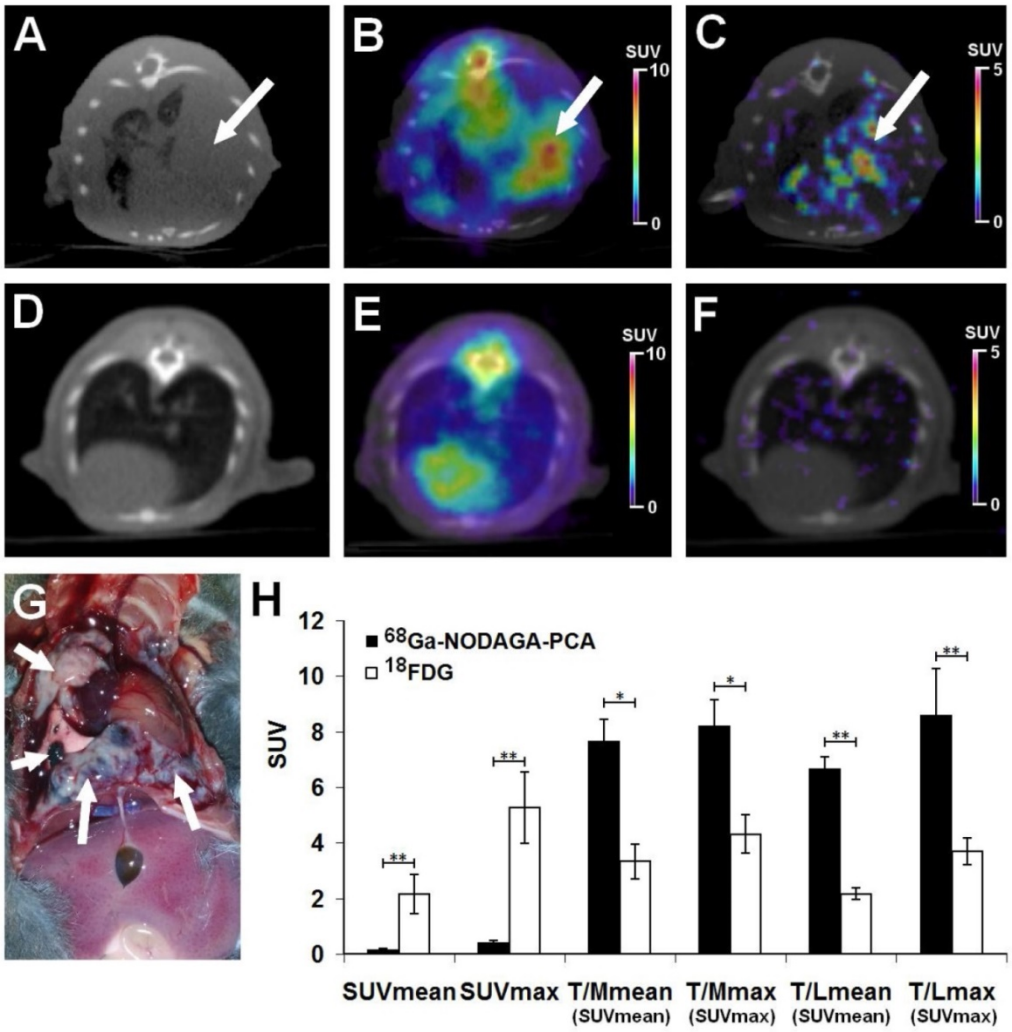

Figure 6. Assessment of ^{68}Ga-NODAGA-PCA and ^{18}FDG uptake in metastatic B16-F10 lesions 20 days after intravenous injection of tumor cells. Upper row: Representative axial CT (A), ^{18}FDG-PET/CT (B) and ^{68}Ga-NODAGA-PCA-PET/CT (C) images of the same tumor-bearing mouse. White arrows: metastatic B16-F10 lesions in the lung. Middle row: Representative axial CT (D), ^{18}FDG-PET/CT (E) and ^{68}Ga-NODAGA-PCA-PET/CT (F) images of a healthy control mouse. Lower row: metastatic B16-F10 lesions (white arrows) 20 days after tumor cell injection (G) and quantitative analysis of *in vivo* tracer uptake data (H) in B16-F10 tumors for ^{68}Ga-NODAGA-PCA (n=5) and ^{18}FDG (n=5). Significance level: $p \leq 0.05$ (*); $p \leq 0.01$ (**).

One day after the small animal imaging *ex vivo* biodistribution studies were performed on the same animals. The *in vivo* data correlated with the *ex vivo* results where the B16-F10 tumor-bearing mice were sacrificed and dissected 90 or 60 min after the injection of ^{68}Ga-NODAGA-PCA or ^{18}FDG, respectively. The radiotracer accumulation of the tumors, muscle and lung was counted with a calibrated gamma counter and DAR values were calculated. The autopsy revealed tumorous infiltration in the lungs (Fig. 6G). Despite the high ^{18}FDG and relatively low ^{68}Ga-NODAGA-PCA accumulation in the metastatic lung melanoma tumors (Table 2), the tumor-to-background (lung, muscle) ratios of ^{68}Ga-NODAGA-PCA uptake were approximately three-fold higher than in case of ^{18}FDG.

Table 2. Tracer uptake (DAR) in *i.v.* induced B16-F10 lung tumors 20±2 days after tumor cell inoculation. Significance level between ^{68}Ga-NODAGA-PCA and ^{18}FDG data: $p \leq 0.05$ (*); $p \leq 0.01$ (**).

Organ/tissue	^{68}Ga-NODAGA-PCA (n=5)	^{18}FDG (n=5)
Tumor (B16-F10)	0.16 ± 0.07**	2.12 ± 0.46
Tumor/Muscle ratio	7.91 ± 1.26*	2.81 ± 0.69
Tumor/Lung ratio	6.73 ± 1.48*	2.53 ± 0.58

Discussion

Considering that the incidence rate of malignant melanoma is increasing, the clinical and preclinical research of this aggressive form of skin cancer is very reasonable. The early detection of primary and metastatic melanoma lesions using non-invasive imaging techniques is critical for the prognosis and the outcome of this malignancy [15]. Among *in vivo* functional imaging techniques in nuclear medicine,

PET is one of the most sophisticated methods that also make it possible to detect tumors and metastases with high accuracy and sensitivity [25]. Among radionuclides used in molecular imaging, the cyclotron independent PET-isotope ^{68}Ga with its near-ideal physical properties offers a well-established chemistry for the labeling of peptides and other small molar-weight biomolecules [20,26,27].

In this study we described the synthesis of the ^{68}Ga-labeled NODAGA-4-Amino-N-(2-diethylaminoethyl) benzamide (^{68}Ga-NODAGA-PCA), which was prepared by the conjugation of 4-Amino-N-(2-diethylaminoethyl) benzamide hydrochloride and NODAGA-NHS ester. The total synthesis time was 15 minutes including the final formulation providing a convenient synthesis timeframe. The radiochemical purity was 98%< and the specific activity was approximately 15 GBq/µmol. Therefore, this radio-synthesis method enables us to produce the melanin specific ^{68}Ga-NODAGA-PCA for *in vitro* and *in vivo* applications easily with high specific activity and radiochemical purity.

The melanin specificity of ^{68}Ga-NODAGA-PCA was investigated under *in vitro* conditions using melanin positive B16-F10 and melanin negative Melur cell lines. The ^{68}Ga-NODAGA-PCA uptake in melanin containing B16-F10 cells was significantly higher than in amelanotic Melur cells at both (30 and 90 min) time points. Earlier it was reported that a radiotracer with similar chemical structure – namely ^{68}Ga-SCN-DOTA-PCA accumulated in B16-F10 cells in a time-dependent manner [13,14]. Our *in vitro* measurements strengthen this observation, due to it was found an increasing accumulation of ^{68}Ga-NODAGA-PCA in B16-F10 cells, but this difference was not significant. Our cellular experiments confirmed the melanin binding specificity of the ^{68}Ga-NODAGA-PCA. Kim et al. [13,14] also found that the radiolabeled benzamide derivatives (*e.g.* ^{68}Ga-SCN-DOTA-PCA, ^{68}Ga-SCN-NOTA-BZA) specifically bind to the melanin pigment or melanin producing B16-F10 melanoma cells. Furthermore, they found elevated radiotracer uptake in B16-F10 cells after L-tyrosine (crucial for melanin synthesis) treatment. The ^{68}Ga-NODAGA-PCA radiotracer uptake in the melanin positive B16-F10 cell line showed higher values at 30 and 90 min, than the reported *in vitro* cellular uptake of ^{68}Ga-SCN-DOTA-PCA (0,56%±0,02% at 2h) [14]. In addition, we found lower radiotracer uptake in B16-F10 cells than it was reported by Ren et al. using ^{18}F-labeled FBZA (*N*-[2-(diethylamino)ethyl]-4-^{18}F-fluorobenzamide) [28]. After the accumulation studies the efflux of ^{68}Ga-NODAGA-PCA was investigated in both cell lines. To examine the washout kinetics of ^{68}Ga-NODAGA-PCA, B16-F10 and Melur cells after 30 or 90 incubation times were incubated 10 minutes further without radiotracer. We found that the ^{68}Ga-NODAGA-PCA content decreased after 10 min efflux. It was hypothesized that after saturation of melanin-content of the cells, the excess radiotracer can remove from the cells. Nevertheless, the uptake ratios of melanin positive B16-F10 and melanin negative Melur cell lines did not differ significantly from the ratio values at 30 and 90 min accumulation (Fig. 2). Several studies reported that the cellular uptake of benzamide derivatives is mediated by passive diffusion and it is correlated with the log*P* value [14,16,29-31]. The log*P* value of ^{68}Ga-NODAGA-PCA was -2.79±0.10 suggesting that the radiotracer is highly hydrophilic. However, Moins at al. [29] described that the log*P* alone is an insufficient feature to predict the biological behavior of radiolabeled benzamide compound because the lower log*P* value results in lower background in tissues, therefore high tumor/background ratio values. However, to the actual transport process(es) through which benzamide-derivatives enter cells needs to be determined in future investigations.

In vivo and *ex vivo* biodistribution studies on healthy animals demonstrated that the ^{68}Ga-NODAGA-PCA was mainly excreted from the kidney as it was expected by the log*P* value. The accumulation of the radiotracer in other organs was low, moderate accumulation was observed after 90 min incubation time (Fig. 3). These results correlated well with other reports where radiolabeled benzamides that share structural similarities with ^{68}Ga-NODAGA-PCA were investigated [13-15,28,29].

The melanin specificity of ^{68}Ga-NODAGA-PCA was investigated by *in vivo* and *ex vivo* biodistribution studies using subcutaneously growing melanotic B16-F10 (in C57BL/6 mice) and amelanotic Melur tumors (in SCID mice) 20±2 days after tumor cell inoculation. 10-min static PET images were obtained 90 min after the *i.v.* injection of ^{68}Ga-NODAGA-PCA. Subcutaneously growing B16-F10 tumors were clearly visualized in miniPET images with low background accumulation (Fig. 4B,C), and after the quantitative analysis of the images we found that the ^{68}Ga-NODAGA-PCA accumulation in melanin containing B16-F10 tumor was significantly ($p \leq 0.01$) higher than in amelanotic Melur tumor (Fig. 4G). These *in vivo* results was correlated with the *ex vivo* biodistribution studies (Table 1), further confirming the melanin specificity of ^{68}Ga-NODAGA-PCA. Our findings agree with the literature, where benzamide-derivatives labeled with PET isotopes (^{18}F, ^{68}Ga) showed relatively high accumulation in B16 tumors with excellent tumor-to-background contrast

[13-15,28,29].

In our study the melanin specificity of ^{68}Ga-NODAGA-PCA was also investigated in lung metastasis mouse model. This syngenic C57BL/6 animal model is widely used in preclinical melanoma research [32,33]. In this present study we developed lung metastases by intravenous injection of $1x10^5$ B16-F10 melanoma cells. By analyzing the miniPET/CT images metastatic tumor lesions were clearly visualized in the lungs 90 min after ^{68}Ga-NODAGA-PCA injection (Fig. 6C) with low background accumulation. After the quantitative evaluation of the PET images approximately 6-8-fold higher ^{68}Ga-NODAGA-PCA accumulation was observed in B16-F10 metastases than that of the background (lung or muscle) uptake.

Although only moderate accumulation of ^{68}Ga-NODAGA-PCA was found in either the subcutaneously growing B16-F10 tumors (SUVmean: 0.35±0.09, SUVmax: 2.03±0.87) or lung metastases (SUVmean: 0.15±0.04, SUVmax: 0.42±0.06), the low activity of other organs allows of high quality images with low background activity and high tumor-to-muscle or tumor-to-lung ratios. Correspondingly, Kim et al. [14] also found that 2 h after intravenous injection of ^{68}Ga-SCN-DOTA-PCA the tumor-to-muscle ratio was 9.47±2.36, resulting high image contrast.

In other experiments the accumulation of ^{68}Ga-NODAGA-PCA in experimental melanoma tumors was compared to ^{18}FDG by small animal PET imaging. ^{18}FDG is frequently used for diagnosis, staging, and therapy control of malignances [4,34]. However, its non-specific property makes the evaluation of the ^{18}FDG-PET images difficult, because of the relative high background accumulation in metabolically active healthy tissues [8,9]. After the intravenous injection of ^{18}FDG for the detection of experimental tumors, high accumulation was found in both subcutaneously growing amelanotic Melur and melanin containing B16-F10 tumors (Fig. 5) and in B16-F10 lung metastases (Fig. 6). After the quantitative analysis of PET images, B16F-10 melanoma tumors showed significantly ($p \leq 0.01$) higher ^{18}FDG uptake than ^{68}Ga-NODAGA-PCA accumulation. Despite these evidences, when the ^{68}Ga-labeled NODAGA-PCA uptake data of the tumors were compared to the background (muscle or lung) activity, we found these values approximately two- or three-fold higher than that of the ^{18}FDG uptake ratios. Due to the specific binding to melanin and the lower background accumulation, ^{68}Ga-NODAGA-PCA provided better contrast than ^{18}FDG.

Conclusion

In this study, we report the synthesis of ^{68}Ga-NODAGA-PCA. Due to its high selectivity and strong binding affinity to melanin, favorable biodistribution and pharmacokinetics, ^{68}Ga-NODAGA-PCA might be a potential molecular probe for the non-invasive *in vivo* imaging of malignant melanoma tumors and metastases. The chelator-PCA adducts can have an additional potential – the replacement of the diagnostic radiometal with a therapeutic one, these structures can serve as theranostics. With this approach, make use of low background of non-targeted tissues and short effective half-life of these radiotracers, PCA-derived radiopharmaceuticals can play an important role in the treatment of malignant melanomas in the future.

Abbreviations

CBCT: cone-beam computer tomography
^{18}FDG: [^{18}F]Fluoro-2-deoxy-D-glucose
i.v. : intravenous
MeCN: acetonitrile
NHS: N-Hydroxysuccinimide
NODAGA: 1,4,7-triazacyclononane-1-glutaric acid-4,7-acetic acid
PCA: 4-Amino-N-(2-diethylaminoethyl)benzamide (procainamide)
PET: positron emission tomography
RCP: radiochemical purity
s.c. : subcutaneous
TFA: triflouroacetic acid

Acknowledgements

This work was supported by a Bolyai fellowship to GT. Furthermore, by grants from the University of Debrecen, NKFIH (K108308, GINOP-2.3.2-15-2016-00006), the Momentum fellowship of the Hungarian Academy of Sciences and the University of Debrecen. The project is co-financed by the European Union and the European Regional Development Fund.

Competing Interests

The authors have declared that no competing interest exists.

References

1. Uong A, Zon LI. Melanocytes in development and cancer. J Cell Physiol. 2010; 222: 38-41.
2. Janczak M. The role of radiopharmaceuticals in diagnosis of melanoma malignum. Nucl Med Rev Cent East Eur. 2009; 12: 83-8.
3. Sandru A, Voinea S, Panaitescu E, Blidaru A. Survival rates of patients with metastatic malignant melanoma. J Med Life. 2014; 7: 572-6.
4. McIvor J, Siew T, Campbell A, McCarthy M. FDG PET in early stage cutaneous malignant melanoma. J Med Imaging Radiat Oncol. 2014; 58: 149-54.
5. Rodriguez Rivera AM, Alabbas H, Ramjaun A, et al. Value of positron emission tomography scan in stage III cutaneous melanoma: a systematic review and meta-analysis. Surg Oncol. 2014; 23: 11-6.

6. Iagaru A, Quon A, Johnson D, et al. 2-Deoxy-2-[F-18]fluoro-D-glucose positron emission tomography/computed tomography in the management of melanoma. Mol Imaging Biol. 2007; 9: 50-7.
7. Kwee TC, Basu S, Saboury B, et al. A new dimension of FDG-PET interpretation: assessment of tumor biology. Eur J Nucl Med Mol Imaging. 2011; 38: 1158-70.
8. Beadsmoore C, Newman D, MacIver D, et al. Positron Emission Tomography Computed Tomography: A Guide for the General Radiologist. Can Assoc Radiol J. 2015; 66: 332-47.
9. Hess S, Hansson SH, Pedersen KT, et al. FDG-PET/CT in infectious and inflammatory diseases. PET Clin. 2014; 9: 497-519.
10. Olivera ME, Ramírez Rigo MV, Chattah AK, et al. Solution and solid state properties of a set of procaine and procainamide derivatives. Eur J Pharm Sci. 2003; 18: 337-48.
11. Scheinbart LS, Johnson MA, Gross LA, et al. Procainamide inhibits DNA methyltransferase in a human T cell line. J Rheumatol. 1991; 18: 530-4.
12. Chang CC, Chang CH, Shen CC, et al. Synthesis and characterization of a novel radioiodinated phenylacetamide and its homolog as theranostic agents for malignant melanoma. Eur J Pharm Sci. 2016; 81: 201-9.
13. Kim HJ, Kim DY, Park JH, et al. Synthesis and characterization of a (68)Ga-labeled N-(2-diethylaminoethyl)benzamide derivative as potential PET probe for malignant melanoma. Bioorg Med Chem. 2012; 20: 4915-20.
14. Kim HJ, Kim DY, Park JH, et al. Synthesis and evaluation of a novel 68Ga-labeled DOTA-benzamide derivative for malignant melanoma imaging. Bioorg Med Chem Lett. 2012; 22: 5288-92.
15. Wu SY, Huang SP, Lo YC, et al. Synthesis and preclinical characterization of [18F]FPBZA: a novel PET probe for melanoma. Biomed Res Int. 2014; 912498.
16. Garg S, Kothari K, Thopate SR, et al. Design, synthesis, and preliminary in vitro and in vivo evaluation of N-(2-diethylaminoethyl)-4-[18F]fluorobenzamide ([18F]-DAFBA): A novel potential PET probe to image melanoma tumors. Bioconjug Chem. 2009; 20: 583-90.
17. Feng H, Xia X, Li C, et al. Imaging malignant melanoma with 18F-5-FPN. Eur J Nucl Med Mol Imaging. 2016; 43: 113-22.
18. Decristoforo C. Gallium-68 -- a new opportunity for PET available from a long shelf-life generator - automation and applications. Curr Radiopharm. 2012; 5: 212-20.
19. Rösch F. Past, present and future of 68Ga/68Ge generators. Appl Radiat Isot. 2013; 76: 24-30.
20. Velikyan I. Prospective of ^{68}Ga-radiopharmaceutical development. Theranostics. 2014; 4: 47-80.
21. Morgat C, Hindié E, Mishra AK, et al. Gallium-68: chemistry and radiolabeled peptides exploring different oncogenic pathways. Cancer Biother Radiopharm. 2013; 28: 85-97.
22. Wängler C, Wängler B, Lehner S, et al. A universally applicable ^{68}Ga-labeling technique for proteins. J Nucl Med. 2011; 52: 586-91.
23. Lajtos I, Emri M, Kis SA, et al. Performance Evaluation and Optimization of the MiniPET-II Scanner. Nucl Instrum Methods. 2013; 707: 26-34.
24. Máté G, Kertész I, Enyedi KN, et al. In vivo imaging of Aminopeptidase N (CD13) receptors in experimental renal tumors using the novel radiotracer (68)Ga-NOTA-c(NGR). Eur J Pharm Sci. 2015; 69: 61-71.
25. Wester HJ. Nuclear imaging probes, from bench to bedside. Clin Cancer Res. 2007; 13: 3470-81.
26. Smith DL, Breeman WA, Sims-Mourtada J. The untapped potential of Gallium 68-PET, the next wave of ^{68}Ga-agents. Appl Radiat Isot. 2013; 76: 14-23.
27. Banerjee SR, Pomper MG. Clinical applications of Gallium-68. Appl Radiat Isot. 2013; 76: 2-13.
28. Ren G, Miao Z, Liu H, et al. Melanin-targeted preclinical PET imaging of melanoma metastasis. J Nucl Med. 2009; 50: 1692-9.
29. Moins N, Papon J, Seguin H, et al. Synthesis, characterization and comparative biodistribution of a new series of p-Iodine-125 benzamides as potential melanoma imaging agents. Nucl Med Biol. 2001; 28: 799-808.
30. Wolf M, Bauder-Wüst U, Mohamed A, et al. Alkylating benzamides with melanoma cytotoxicity. Melanoma Research. 2004; 14: 353-60.
31. Wolf M, Bauder-Wüst U, Haberkorn U, et al. Alkylating benzamides with melanoma cytotoxicity: role of melnon, tyrosinase, intracellular pH and DNA interaction. Melanoma Research. 2005; 15: 383-91.
32. Vantyghem SA, Postenka CO, Chambers AF. Estrous cycle influences organ-specific metastasis of B16F10 melanoma cells. Cancer Res. 2003; 63: 4763-5.
33. Winkelmann CT, Figueroa SD, Rold TL, et al. Microimaging characterization of a B16-F10 melanoma metastasis mouse model. Mol Imaging. 2006; 5: 105-14.
34. Gambhir SS. Molecular imaging of cancer with positron emission tomography. Nat Rev Cancer. 2002; 2: 683-93.